*Radio Science*, Volume 23, Number 3, Pages 299–307, May–June 1988

# Ionospheric imaging using computerized tomography

Jeffrey R. Austen, Steven J. Franke, and C. H. Liu

Department of Electrical and Computer Engineering, University of Illinois at Urbana-Champaign

(Received October 1, 1987; revised January 12, 1988; accepted January 20, 1988.)

Computerized tomography (CT) techniques can be used to produce a two-dimensional image of the electron density in the ionosphere. The CT problem requires that the measured data be the line integral through the medium of the unknown parameter; transionospheric satellite beacon total electron content data recorded simultaneously at multiple ground stations fulfill this requirement. In this paper the CT problem is formulated as it applies to ionospheric imaging and limitations of the technique are investigated. Simulations are performed assuming a 1000-km-altitude polar-orbiting satellite and both five and three ground stations; the results demonstrate the feasibility of this technique.

## INTRODUCTION

Total electron content (TEC), the content of a unit cross-section column through the ionosphere, has been measured for many years using Faraday rotation and differential Doppler techniques [e.g., Garriott et al., 1970]. These measurements provide important information about the ionosphere through the study of the temporal and spatial variations of the column electron content. Indeed, multistation TEC data have been used to study horizontal (latitudinal as well as longitudinal) variations of ionospheric structures [Leitinger et al., 1984]. However, since TEC represents the integral of the electron density along the propagation path, the information about the spatial variation of the electron density along the path caused by the irregular structures cannot be recovered using the conventional procedure to process TEC data. In this paper, we present a new method for processing TEC data obtained simultaneously at several receiving stations. This method has the potential for obtaining a two-dimensional "picture" of the ionosphere structures, including both the horizontal and vertical variations. The method is based on the technique of computerized tomography (CT). CT techniques can be used when the line integral of the parameter to be determined (for example, attenuation or electron density) is the measured data. In order for this method to work well the data must be collected for paths that pass through the region of interest in many positions and orientations. CT techniques have had a revolutionary impact in the field of medical diagnostic imaging and are now used routinely to produce high-quality images of a cross section of the human body [Herman, 1980]. Recently, CT techniques have been applied to the study of ocean structures [Munk and Wunsch, 1979] and geological formations [Dines and Lytle, 1979]. In this paper we will examine the application of CT techniques to the study of the ionosphere and will present some results obtained from computer simulations.



Paper number 8S0079.
0048-6604/88/008S-0079$08.00

## THEORY

An easily measured parameter of the ionosphere is the total electron content (TEC), which is the number of free electrons in a column of unit cross-sectional area.

$$\mathrm{TEC} = \int_p N(s)\,ds \tag{1}$$

where N(s) is the electron content per unit volume, and p is the propagation path between the source and the detector. In this paper the TEC values are not corrected for the angle between the path and zenith but are the "slant TEC" values. The techniques for measuring TEC, such as Faraday rotation and differential Doppler, are well known; for the following discussion it is assumed that an appropriate technique has been used to measure the TEC. Geometric optics is assumed and in addition, we assume that the carrier frequencies used to measure the TEC are high enough so that the path p is a straight line joining the source and receiver.

Computerized tomography is the process of reconstructing an image from a series of its projections. Bates et al. [1983] and Scudder [1978] review the development of CT, its principles, current techniques, and applications. The algorithms used for CT can be divided into two classes: transform methods and finite series expansion methods. They are reviewed by Lewitt [1983] and Censor [1983], respectively. Because the ionospheric imaging problem does not involve a geometry that lends itself to a direct application of the transform methods, the finite series expansion technique which can be used for any geometry will be investigated.

Let $f(r,\phi)$, where r and $\phi$ are coordinates in a two-dimensional coordinate system with the origin at the center of the Earth, represent the electron density in a planar cross section of the ionosphere and let $p_i$ be the path that ray i takes through the ionosphere. We will restrict our attention to the case where all paths lie in the plane. The measured parameter, $y_i$, is defined as the line integral through the ionosphere along path $p_i$; there are $N_p$ paths:

$$y_i = \int_{p_i} f(r,\phi)\,ds \qquad i = 1,\ldots,N_p \tag{2}$$

Note that $y_i$ is the TEC along path $p_i$. The actual density, $f(r,\phi)$, can be approximated by using a set of $N_b$ basis functions $\{b_j(r,\phi)\}$

$$f(r,\phi) \approx \hat{f}(r,\phi) = \sum_{j=1}^{N_b} x_j b_j(r,\phi) \tag{3}$$

where $x_j$ is the weighting coefficient for $b_j(r,\phi)$. Substituting (3) into (2) produces

$$y_i = \int_{p_i} f(r,\phi)\,ds \approx \int_{p_i} \sum_{j=1}^{N_b} x_j b_j(r,\phi)\,ds =$$

$$\sum_{j=1}^{N_b} x_j \int_{p_i} b_j(r,\phi)\,ds = \sum_{j=1}^{N_b} D_{ij} x_j \tag{4}$$

where the $D_{ij}$ are the elements of a two-dimensional matrix that depends only on the choice of paths and basis functions, i.e.,

$$D_{ij} = \int_{p_i} b_j(r,\phi)\,ds \tag{5}$$

Let $e_i$ be an error term due to the approximate nature of the series expansion and inaccuracy in measurements. Then,

$$y_i = \sum_{j=1}^{N_b} D_{ij} x_j + e_i \tag{6a}$$

or, in matrix notation,

$$Y = DX + E \tag{6b}$$

The error term can be explicitly incorporated into the system of equations and solved for, as in Radcliff and Balanis [1979], but in doing so one must solve a much larger system of equations. For computer simulations where the data are noiseless and the basis set can be chosen to accurately represent the true electron density distribution, this error term can be neglected.

In many CT systems the region being imaged is divided into small rectangular elements called pixels. With this choice the value of each pixel is simply the density of the object in that region. Due to the geometry involved in ionospheric imaging, the pixels will be sections of annuli instead of rectangles (see Figure 1). To represent the pixels a set of basis functions is defined such that

$$b_j(r,\phi) = \begin{cases} 1, \text{ if } (r,\phi) \text{ is inside the jth pixel} \\ 0, \text{ otherwise} \end{cases} \tag{7}$$

With this choice, the weighting factors $x_j$ can be interpreted as the average electron density in the jth pixel.

Once the basis functions are chosen and the ray paths are known, (5) can be evaluated to obtain **D**. The problem is then reduced to solving (6) where X is the unknown and Y is the known data, subject to some constraint on X and the error term, E.

There are many different techniques for solving (6). Row action techniques are a class of iterative procedures in which only one row of **D** is used at a time and the values of **D** are not changed [Censor, 1981]; these techniques can be very attractive when computer memory is limited. One such technique is called the algebraic reconstruction technique (ART). The kth iteration of this algorithm computes the difference between Y and $Y^k$ where $Y^k$ is obtained by using the current estimate of the solution, $X^k$, in (6). A correction derived from this difference is then distributed over $X^k$ to obtain $X^{k+1}$; after many iterations the result converges to a solution of (6). An initial guess, $X^0$ is required before the iteration begins. For the kth iteration,

$$X^{k+1} = X^k + \lambda_k \frac{y_i - \sum_{j=1}^{N_b} D_{ij} x_j^k}{\sum_{j=1}^{N_b} D_{ij} D_{ij}} D_i \tag{8}$$

where $\mathbf{D}_i$ is the ith row of **D** and $i = k \bmod N_p$. The values $\lambda_k$ are relaxation parameters, a sequence of real numbers usually confined to the interval $0 < \lambda_k < 2$. Often $\lambda_k$ is chosen to be the same for all k. When using noisy data the quality of the reconstruction can be greatly improved with the proper choice of relaxation parameters [Radcliff and Balanis, 1979]. When applied to a consistent set of equations, this technique converges to the minimum norm solution. A common modification to ART, when there is a physical basis for doing so, is to restrict the values of X to be nonnegative.

Quadratic optimization techniques minimize a general quadratic function. This includes norm minimization methods, Bayesian reconstruction, and least squares regularization.

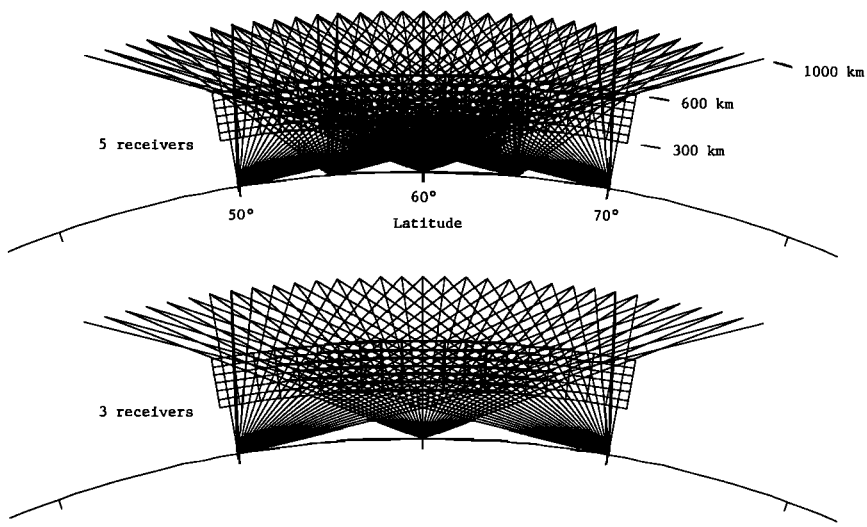


Fig. 1. Geometry plots showing the location of the receivers, satellite positions, the ray paths, and the division of the imaged region into pixels.

Several of these methods are discussed by Herman and Lent [1976]. One of these techniques, the simultaneous iterative reconstruction technique (SIRT) algorithm computes error in the same manner as ART (the right-hand term of (8)) but only corrects the X array after the errors for all the ray paths have been computed.

Noniterative techniques involve choosing a basis function set so that the solution of the resulting matrix equation is computationally feasible [Munk and Wunsch, 1979]. These techniques are discussed by Herman [1980] and Buonocore et al. [1981]. Another possibility is to directly compute the Moore-Penrose pseudo-inverse of D and use it to obtain the least squares error minimum norm solution. In the process of computing the pseudo-inverse, the singular values of D are computed and they may be useful for comparing the "quality" of different choices of basis function sets and ray path geometries. The pseudo-inverse method is only feasible when the number of rays and pixels is relatively small; hence it is not seriously considered for problems such as medical tomography. However, it may be applicable to the ionospheric imaging problem.

There are several geometrical considerations for the reconstruction problem. In order to avoid spatial undersampling the spacing of the rays must be small enough so that adjacent rays go through the same or adjacent pixels. For the type of geometry shown in Figure 1 the most stringent sampling requirement occurs for the highest pixels directly above a receiver. At this location the horizontal distance between rays must be equal to or less than the horizontal dimension of the pixels.

Another consideration involves the sides of the region being imaged. The electron density outside the sides of the region is unknown, but not insignificant, so that any rays that passed through the sides of the region would have an unknown contribution to the TEC. Therefore no rays that pass through the sides of the region of interest are used in the reconstruction. A similar argument can be made concerning the choice of upper and lower bounds of the imaged region: the contribution to TEC of the area outside the imaged region must be negligible. Because of the prohibition on rays passing through the sides of the region the ray coverage near the sides is poor and the quality of the reconstruction will suffer near the sides of the imaged region. For real data the geometry will be three-dimensional. In that case it must be assumed that the electron density does not vary appreciably for some distance perpendicular to the image plane.

## EXAMPLES

To demonstrate the feasibility of this technique a number of computer simulations are performed in which TEC data are obtained by computing the line integral (equation (1)) through a model of the ionosphere and then those data are used to perform the reconstruction (equation (6)). The reconstruction can then be compared with the original model.

The image dimensions are six pixels in the vertical direction and 20 pixels horizontally for a total of 120 pixels. Each pixel is 50 km high and approximately 125 km wide; the total region imaged is 300 km by approximately 2500 km. (Because a spherical geometry is used the horizontal dimensions vary with altitude.) We note that these dimensions do not necessarily represent the ultimate resolution that can be obtained with the technique. The top and bottom heights of the imaged region are chosen so that it contains all of the region where there is significant electron density; for this case

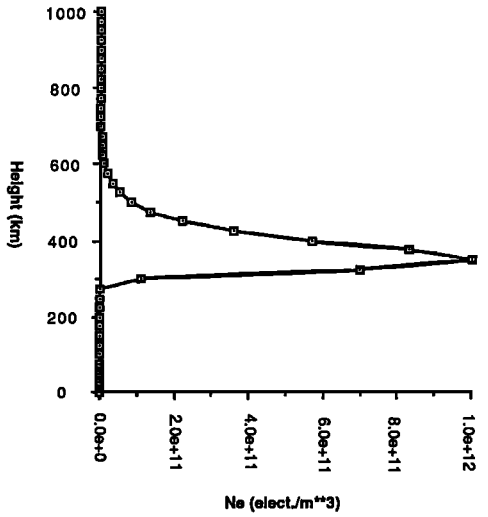


Fig. 2. The background profile used in the ionospheric models.

the bottom is 300 km and the top is 600 km altitude. The edges are chosen to be at latitudes of 70.5° and 49.5°, just beyond the location of the farthest receivers. A satellite in a circular polar orbit at an altitude of 1000 km is used as a signal source. The TEC data are sampled once every 1° of satellite motion; this is equivalent to a receiver that samples TEC every 17.5 s. Two geometries were tested, the only differences being the number of receivers. The first geometry has five receivers which are located at latitudes of 50°, 55°, 60°, 65°, and 70°; the second geometry has three receivers located at 50°, 60°, and 70° latitude. These geometries are shown in Figure 1.

There are two components to the ionospheric model: background profile and irregularities. The background profile is a Chapman layer with parameters Nmax = $10^{12}$ electrons/$m^3$, scale height = 25 km, and height of the peak = 350 km. A plot of the profile is shown in Figure 2. The irregularities are a combination of large and small Gaussian depletions

$$d(x',z') = 1.0 - 0.9 * \exp\left[ - \left\{ \left(\frac{x'}{major}\right)^2 + \left(\frac{z'}{minor}\right)^2 \right\} \right] \quad (9)$$

where x' and z' are a rotated coordinate system and "major" and "minor" are the scale sizes. The small depletions are circular with a scale size of 100 km. The large depletions are

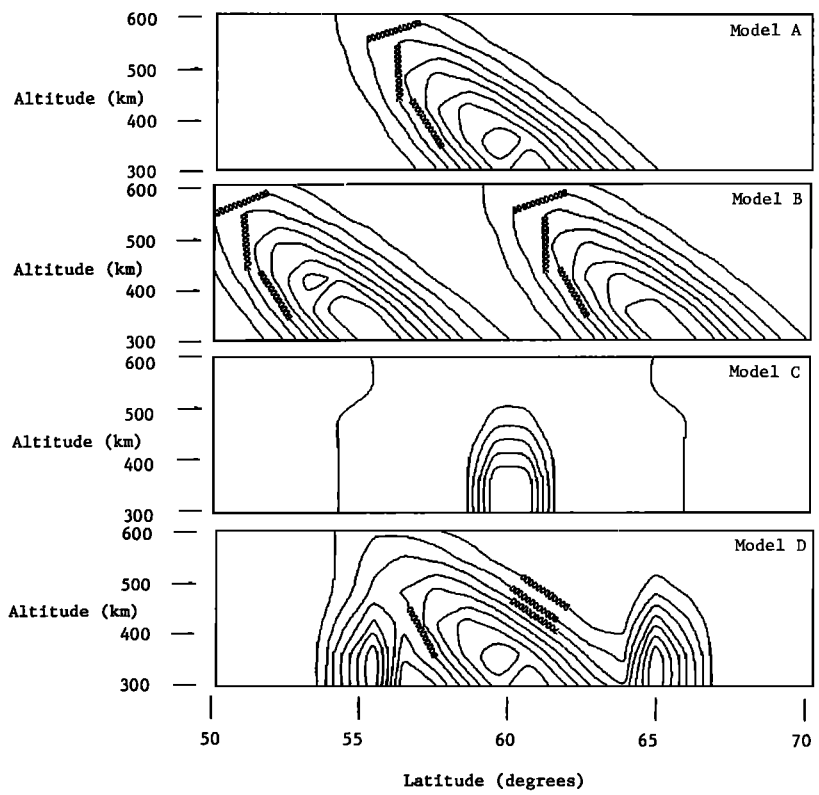


Fig. 3. The irregularities used in the ionospheric models.

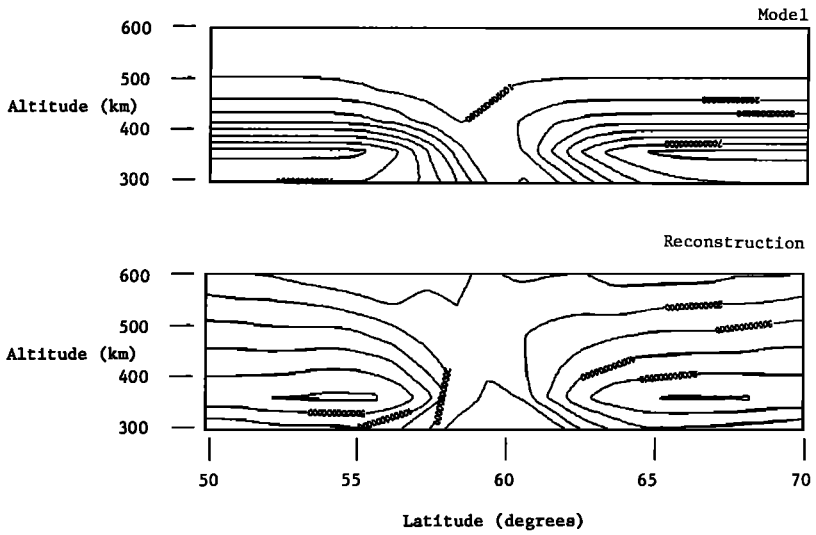


Fig. 4. Ionospheric model A and the reconstruction obtained with the five-receiver geometry.

elongated with the major axis tilted 45° from vertical; the scale size for the major axis is 500 km and for the minor axis is 100 km. The four models created using these elements are shown in Figure 3. Model A consists of one large depletion in the center of the region; model B consists of two large depletions. Model C consists of one small depletion in the center. Model D consists of one large depletion in the center, as in model A, with two small depletions, one on each side of the large depletion. The ionospheric models are obtained by multiplying the background profile by the irregularities.

For the reconstructions that follow, a sequence of 30 iterations of the the SIRT algorithm with a relaxation parameter of 0.1 is used to obtain the reconstructed image. A ray weighting scheme similar to that of Dines and Lytle [1979] is employed in which the correction from each ray is divided by the total length of the ray through the imaged region. With this correction each ray has an equally weighted contribution to the total error. The initial guess is determined by computing the average electron density value by averaging all the TEC data together and assuming a triangular-shaped profile with the peak level at 375 km. No noise was added to the data for these reconstructions.

The four electron density models are used with the five-receiver geometry. Figures 4 through 7 show the ionospheric models and the reconstructions obtained. For the more complicated models (Figures 5 and 7) the three-receiver reconstructions are also shown. Care must be taken when interpreting the plots because the existence of the background profile causes the contour lines to not show the irregularities clearly. For example, compare model A of Figure 3 (irregularity only) with the model of Figure 4 (irregularity and background). In all cases the position, orientation, size and strength of the irregularities are reconstructed with reasonable accuracy. Note that the quality of the three-receiver reconstructions is similar to the quality of those done with all five receivers; this is also true of the three-receiver reconstructions for models A and C (not shown). It should be noted that the background profile of the reconstruction is not equal to the profile of the model, but is that of the initial guess. This is a result of having incomplete data. Due to physical constraints, for example, not being able to place a receiver at a fixed point 400 km above the Earth, no ray paths exist which contain information on the vertical profile. These ray paths would correspond to lines that are nearly horizontal in Figure 1. This limitation can be partially overcome by employing a good knowledge of the background profile obtained from other investigations. Additionally, it is possible to incorporate data from other sources, such as incoherent scatter radar or in-situ probes, into the reconstruction algorithm.

Figure 8 shows the TEC data associated with model D. Because the CT technique reconstructs an image such that the TEC calculated from the image is equal to the TEC data input to the algorithm, a good agreement on the plots is expected. In the figure the true vertical TEC, obtained from the ionospheric model, is compared with the vertical TEC of the reconstructed image and that derived directly from the slant TEC. The vertical TEC of the reconstructed image is obtained by adding up the electron density in each pixel of a column of pixels and multiplying by the height of the column. The vertical TEC curves for each receiver are estimated by dividing the slant TEC (measured data) by the secant of the zenith angle of the ray at 350 km altitude. This is the conventional approach to estimating the vertical TEC. Note that in general

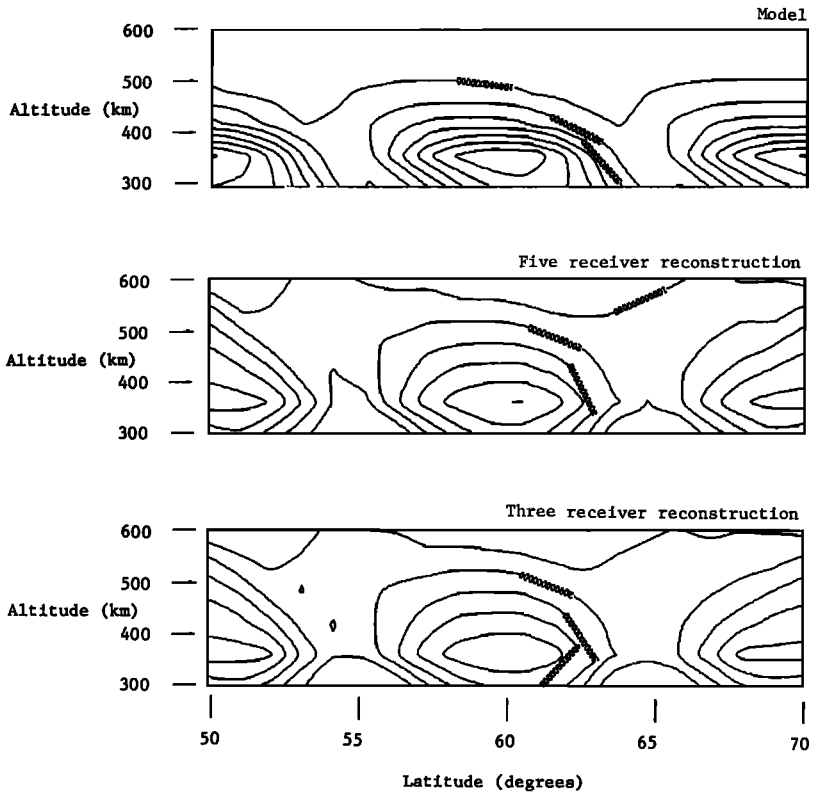


Fig. 5. Ionospheric model B and the reconstructions obtained with the five- and three-receiver geometries.

the vertical TEC derived from the CT technique agrees much better with the true vertical TEC than does the curve derived from any of the individual receivers.

In order to examine the effects of the initial guess, noise, algorithms, relaxation parameters, and number of iterations some "special case" reconstructions are done. The effects of different initial guesses on the reconstruction are shown in Figure 9. In both examples the irregularity is reconstructed

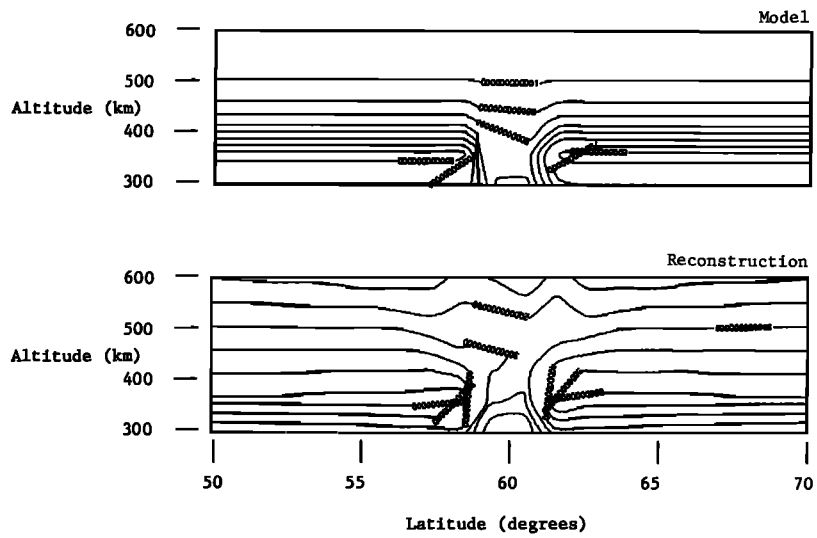


Fig. 6. Ionospheric model C and the reconstruction obtained with the five-receiver geometry.

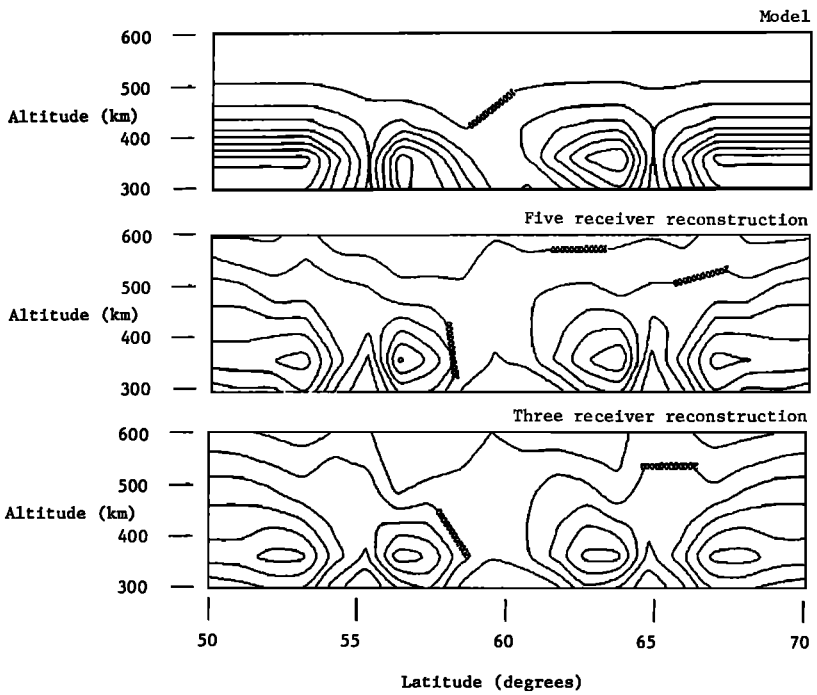


Fig. 7. Ionospheric model D and the reconstructions obtained with the five- and three-receiver geometries.

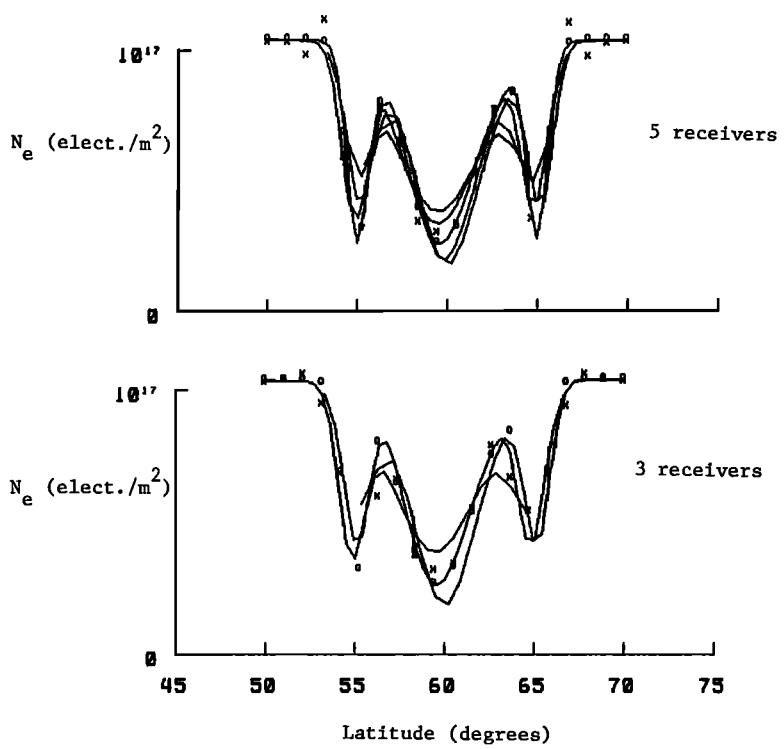


Fig. 8. Vertical TEC plots of the data (lines), model (circles), and reconstruction (crosses). Vertical TEC for the data is obtained by dividing the slant TEC by the secant of the zenith angle measured at 350 km altitude.

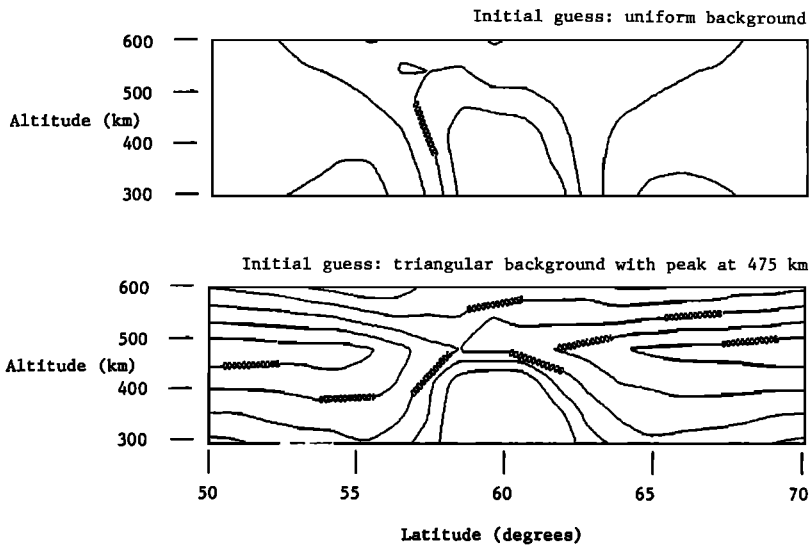


Fig. 9. Reconstructions produced with varying initial guess. The model is shown in Figure 4.

and the background profile is close to the initial guess. Figure 10 shows the reconstruction for a case where 5% Gaussian noise is superimposed on the TEC data. The initial guess was the same as in Figure 4. Comparing it with Figure 4 shows that the noise has little effect on the reconstruction.

Several combinations of the number of iterations and relaxation parameters were used with both the ART and SIRT algorithms. The quality of the reconstruction does not vary appreciably for reasonable choices of the parameters. As expected, as the relaxation parameter is reduced the number of iterations must be increased in order to achieve the same reconstruction quality. When the relaxation parameter is greater than 0.3 the SIRT algorithm fails to converge. In the presence of noise there is expected to be an optimum choice for these parameters [Radcliff and Balanis, 1979].

## DISCUSSION

The theory of computerized tomography as applied to the problem of ionospheric imaging has been presented, and the problems and limitations of this technique have been outlined. A computer program has been developed which both generates the TEC data from a mathematical model of the ionosphere and processes those data using CT algorithms. The results from simulations show a good correlation between the model electron density and the electron density computed using CT to process the TEC data. The vertical TEC of the reconstructed image is shown to match the vertical TEC of the model quite well and the position, size, and orientation of the irregularities are reconstructed accurately. We believe the CT technique offers the first technique for combining TEC data from multiple stations in a self-consistent manner in order to obtain the "true" vertical TEC without using the ad hoc secant $\chi$ corrections. A limitation of this technique in determining the vertical profile has been shown to exist, but further study may reveal solutions to that problem. Our results demonstrate that multistation TEC data that are obtained routinely from Navy Navigation Satellite System or Global Positioning System satellites can be used to reconstruct the two-dimensional picture of the ionosphere with realistic receiving station

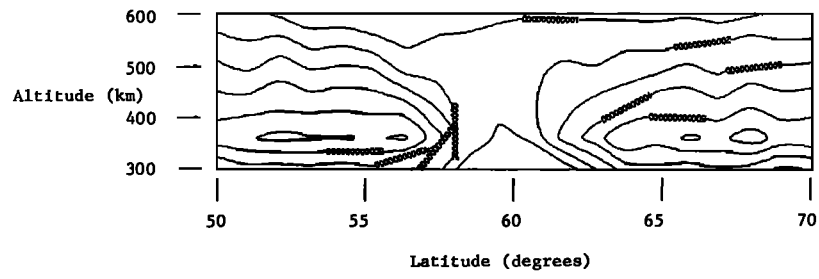


Fig. 10. Reconstruction with 5% noise superimposed on the TEC data. The model is shown in Figure 4.

geometries. For example, the geometry modeled in this paper is similar to an existing network of geodetic Doppler receivers in Europe [Leitinger et al., 1984].

Before this technique can be used on real data with confidence, more study is needed. There are many other reconstruction techniques that may be used. Several modifications of the ART algorithm which make it more robust in the presence of noise have been studied [Radcliff and Balanis, 1979; Balanis and Bentley, 1986]; these algorithms may prove more suitable for ionospheric usage than ART or SIRT. The effects of noise (both Gaussian noise and other forms of "noise" such as a gravity wave propagating through the region during the time that measurements are being taken) need further study. Also, many techniques of measuring TEC only determine it to within an additive constant ("constant of integration") and the CT algorithm requires knowledge of that constant; this problem is currently being studied by the authors. The inability of CT to resolve the vertical profile of the electron density is not a limitation of the technique itself, but a result of missing data. Methods of incorporating other sources of data into the CT algorithms are being investigated.

*Acknowledgments.* This research was supported in part by grant ATM 84-14134 from the Atmospheric Research Section, National Science Foundation. Computational resources were provided by the National Center for Supercomputing Applications.

## REFERENCES

Balanis, C. A., and J. D. Bentley, Algorithm and filter selection in geophysical tomography, *IEEE Trans. Geosci. Remote Sens., GE-24*(6), 983–996, 1986.

Bates, R. H. T., K. L. Garden, and T. M. Peters, Overview of computerized tomography with emphasis on future developments, *Proc. IEEE, 71*(3), 356–372, 1983.

Buonocore, M. H., W. R. Brody, and A. Macovski, Fast minimum variance estimator for limited angle CT image reconstruction, *Med. Phys., 8*(5), 695–702, 1981.

Censor, Y., Row-action methods for huge and sparse systems and their applications, *SIAM Rev., 23*(4), 444–466, 1981.

Censor, Y., Finite series-expansion reconstruction methods, *Proc. IEEE, 71*(3), 409–419, 1983.

Dines, K. A., and R. J. Lytle, Computerized geophysical tomography, *Proc. IEEE, 67*(7), 1065–1073, 1979.

Garriott, O. K., A. V. daRosa, and W. J. Ross, Electron content obtained from Faraday rotation and phase path length variations, *J. Atmos. Terr. Phys., 32*, 705–727, 1970.

Herman, G. T., *Image Reconstruction From Projections*, Academic, Orlando, Fla., 1980.

Herman, G. T., and A. Lent, Quadratic optimization for image reconstruction, I, *Comput. Graphics Image Process., 5*, 319–332, 1976.

Leitinger, R., G. K. Hartmann, F.-J. Lohmar, and E. Putz, Electron content measurements with geodetic Doppler receivers, *Radio Sci., 19*(3), 789–797, 1984.

Lewitt, R. M., Reconstruction algorithms: Transform methods, *Proc. IEEE, 71*(3), 390–408, 1983.

Munk, W., and C. Wunsch, Ocean acoustic tomography: A scheme for large scale monitoring, *Deep Sea Res., 26A*, 123–161, 1979.

Radcliff, R. D., and C. A. Balanis, Reconstruction algorithms for geophysical applications in noisy environments, *Proc. IEEE, 67*(7), 1060–1064, 1979.

Scudder, H. J., Introduction to computer aided tomography, *Proc. IEEE, 66*(6), 628–637, 1978.

J. R. Austen, S. J. Franke, and C. H. Liu, Department of Electrical and Computer Engineering, University of Illinois, 1406 West Green, Urbana, IL 61801.